

Model-Informed Drug Repurposing: Viral Kinetic Modeling to Prioritize Rational Drug Combinations for COVID-19

Michael Dodds¹, Rajesh Krishna¹, Antonio Gonclaves², and Craig Rayner¹

¹Certara LP

²INSERM

June 12, 2020

Abstract

Aim: We hypothesize that the efficacy of COVID-19 therapeutic candidates will be better predicted by understanding their effects at various points on a viral cell cycle, in particular, the specific rate constants, and that drugs acting independently of these specific discrete sites may not yield expected efficacy. We hypothesize that drugs, or combinations of drugs that act at specific multiple sites on the viral life cycle have the highest probability of success in the treatment of early infection phase in COVID-19 patients. **Methods:** Using a target cell limited model structure that had been used to characterize viral load dynamics from COVID-19 patients, we performed simulations to show that combinations of therapeutics targeting specific rate constants have greater probability of efficacy and supportive rationale for clinical trial evaluation. **Results:** Based on the known kinetics of the SARS-CoV-2 life cycle, we rank ordered potential targeted approaches involving repurposed, low-potency agents. We suggest that targeting multiple points central to viral replication within infected host cells or release from those cells is a viable strategy for reducing both viral load and host cell infection. In addition, we observed that the time-window opportunity for a therapeutic intervention to effect duration of viral shedding exceeds the effect on sparing epithelial cells from infection or impact on viral load AUC. Furthermore, the impact on reduction on duration of shedding may extend further in patients who exhibit a prolonged shedder phenotype. **Conclusions:** Our work highlights the use of model-informed tools to better rationalize effective treatments for COVID-19.

Introduction

The ongoing coronavirus pandemic has resulted in more than 7.4 million cases of infection and more than 418,000 deaths worldwide, including more than 115,000 deaths in the US alone as of 11-June-2020 [1,2]. The SARS-CoV-2 virus was subsequently isolated and the disease designated as COVID-19 [1,3,4].

According to the Siddiqui and Mehra typology of COVID-19 disease progression, three distinct phases are evident from the first stage being presented as mild phase and occurring immediately following infection and early disease [5]. During this phase, SARS-CoV-2 multiplies and engages with the host respiratory system. Stage 2 of the clinical progression involves moderate pulmonary involvement wherein infected subjects evidence early stages of viral pneumonia, with more pronounced cough and fever. Stage 3 is the severe form of infection where there is evidence of systemic hyperinflammation. Here, systemic inflammation markers are elevated. Patients progress to shock, vasoplegia, respiratory failure, and cardiopulmonary collapse. This is the phase with overall poor prognosis and recovery [5].

As of 11-June-2020, there were 1166 clinical interventional studies registered in clinicaltrials.gov with therapies targeting COVID-19. Due to the studies being on the pandemic frontlines, many of these studies are not appropriately designed randomized placebo-controlled clinical trials and often targeted patients with COVID-19 that are hospitalized and were diagnosed with severe form [6-9].

In many cases, exploration of treatment options for COVID-19 has been occurring without consideration of biological or pharmacological plausibility for the therapeutic to work, or the stage of infection the patient is in. We hypothesize that, considering not only the timing of intervention, but more importantly dose and schedule of these interventions, treatments given alone or in combination matched to the cell cycle of the virus and the purported windows of opportunity, will yield clinically significant reductions in viral loads and associated efficacy. This cell cycle dependency of treatment options forms the central premise of our investigations and is further conceptualized in **Figure 1**.

There are various population level viral cell cycle models available in the literature. These vary by the complexity of the models, ranging from the most parsimonious target cell limited model to the most sophisticated yet complex multi-scale models that describe virus-host interactions [10-12]. These models were used to characterize a variety of viruses including HIV, HCV, and Influenza A. We believe that viral cell cycle in basic terms would be adequate to test the impact of the currently envisaged antiviral armamentarium. However, as models evolve, a fuller quantitative and systems pharmacology (QSP) model might provide a scaffold for the generation of testable hypotheses incorporating interventions impacting downstream host-inflammatory pathways. We consider our efforts as a parsimonious first module to inform and inspire more comprehensive QSP strategies, not only for COVID-19 but for emerging viruses in general.

In simple terms, the target cell-limited model integrates four entities: uninfected susceptible epithelial target cells (T), latently infected cells ($I1$), productively infected cells ($I2$), and the virus load (V) and is described by a system of nonlinear ordinary differential equations [13]. Given the timescale of the infection, we neglect target cell proliferation and natural death, and focus on the process of epithelial cell depletion (T) by virus infection. When a virus interacts with an uninfected target cell at a defined infection rate, β , then the target cells will become infected ($I1$) and remain so during an incubation period. These cells, in turn, convert to productively infected cells ($I2$) at a rate, k . These cells then produce new virions (V) with a defined production rate, ρ . Simultaneously, productively infected cells die at a certain rate, δ . Circulating virions are then cleared at a certain rate, c , from the body or go on to infect new cells as above. Based on the dynamics of the cell model and the associated mechanisms of actions of the currently experimented drugs for SARS-CoV-2 infection, we classify treatments to potentially affect one or more of the five different distinct check points in this model: β , k , ρ , δ , c (**Figure 1**). We describe a model-informed analytical framework that yields predictions on the most viable combinations of drugs matched by phase of clinical progression.

Materials and methods

Model

We used a “target-cell limited” model with an eclipse phase based on an analysis published by Goncalves et.al., 2020 [14] that was used to characterize the viral load dynamics of 13 hospitalized patients from frequent nasopharyngeal swabs. Readers are directed to that publication for details on the analysis, assumptions and data. The authors performed a similar analysis presented here, focusing on specific drug effects and intervention time.

Specific model parameters for this exercise were: $V_0=0.1$ #/mL, $T_0=1.33E^5$ #/mL, $k=3$ 1/d, $\delta=0.60$ 1/d, $\beta=2.21E-5$ mL/#/day, $\rho=22.7$ 1/d, $c=10$ 1/d. For state variables representing cells and virions, the meaning of “#” was “cells” and “copies”, respectively. The parameter β was derived from the reported R_0 of 8.6 with the equation $\beta = R_0 * \delta * c / [T_0 * (\rho - R_0 * \delta)]$.

Intervention effects

Interventions were posited for the targets in the viral life cycle given in **Figure 1**. Intervention effects were modeled as inhibitory functions for β , k , ρ (e.g. $\beta * [1 - I_{max}(t)]$) and stimulatory function for δ , c (e.g. $\delta * [1 + S_{max}(t)]$). $S_{max}(t)$ and $I_{max}(t)$ were treated as step (Heaviside) functions with onset at times relative to the approximate viral peak, estimated as 9 days post infection: -6, -3, 0, +3, +6 days. Intervention at viral peak -6 and -3 days represent cases of pre- and post-exposure prophylaxis; intervention at 0 and +3 days represent cases of symptomatic presentation; intervention at +6 days represent cases of advanced infection.

Specific values of inhibition (I_{max}) and stimulation (S_{max}) were selected with the intention to “blanket” the space of pharmaceutical intervention from low to very high potency **Supplemental Figure 1** reports the specific values, noting that the choices are interconvertible and can be expressed in terms of drug effect, I_{max} or S_{max} :

$$\log_{10} \text{ Drug Effect} = \log_{10}[S_{max}+1] = -\log_{10}[1-I_{max}]$$

With this particular formation, a fair assessment of e.g. 1 \log_{10} change in an inhibitory versus stimulatory effects can be made. Additionally, the specific values of individual effect (0, 0.333, 0.667, 1, 1.33, 1.67, 2 \log_{10} change) can be summed for easy comparison. For example, a single effect with 1 \log_{10} change (90% inhibition or 9-fold stimulation) can be compared to an intervention with three effects each with 0.333 \log_{10} change (53.6% inhibition or 1.15-fold simulation, each) fairly. If the three effects are strictly additive, then the total effect is $100*(1-(1-0.536)^3)=90\%$ and would result in the same effect as a monotherapy effect of 90%, *if* the effect is additive and targets the same pathway. In these simulations, different pathways are explicitly targeted and the model is nonlinear (second-order) in the dynamics. Thus, difference in simulation outcome for two interventions with the same summed \log_{10} change effect describe synergy and anergy of targeting different pathways.

Simulations

Simulations were conducted in *R* (3.6.1) using the *RxODE*(0.9.2) package for numerical integration and the *tidyverse*(1.2.1) family of packages. A R script reproducing these results is provided in **Supplemental Script 1**.

Each of the five checkpoints (β , k , ρ , δ , c) were probed with seven drug effect levels (0, 0.333, 0.667, 1, 1.33, 1.67, 2 \log_{10} change) for a total of 16,797 simulation conditions. Each condition was replicated over five intervention times (viral peak at 9 -6, -3, 0, +3, +6 days) for a total of 84,035 condition-times. However, simulations were reduced to cases with summed intervention effect between 0.333 and 2 \log_{10} change, reducing the total simulations to 2,310 intervention conditions.

Endpoints and Metrics

Viral load dynamics has been elevated to surrogate status in the management of HIV by the FDA, and is aligned with clinical outcome for respiratory viral infections including seasonal and emerging influenza strains in various populations [15] and correlated with clinical outcome in SARS-CoV-2 infection [16]. Duration of viral shedding and impact of therapeutic interventions has been linked to transmission and health economic models, demonstrating indirect benefits of individual treatment to societal outcomes for pandemic influenza [17]. Such endpoints have been critical importance in informing procurement and deployment decisions for interventions within health care systems during outbreak scenarios. Viral kinetic modelling has also been extensively used to support drug development decisions in the respiratory virus space [18].

Nevertheless it is unknown what specific features of SARS-CoV-2 infection captured in the existing model relate to individual patient outcome and also transmission of infection.

As such, we generated three key metrics for each simulation case:

Viral Load Area Under the Curve (AUC):

The viral load AUC is calculated as the area under the viral load, V , time curve (copies/mL*day). This metric summarizes the total exposure to SARS-CoV-2 virions. This endpoint may have prognostic correlation to clinical outcome, however because it is highly dependent on the pre-intervention viral load values it is, consequently, insensitive to treatment interventions that occur beyond the peak viral load time. Moreover, because pre-intervention loads are seldom measured experimentally, it remains a theoretical phase, that provides important insights into pre (PrEP) and post exposure prophylaxis (PEP) strategies.

Duration of Viral Shedding:

The duration of time (days) for which the virus concentration, V , exceeds 100 copies/mL, which is often the lower limit of detection for qPCR assays for SARS-CoV-2 [19]. This duration of viral shedding metric summarizes the amount of time virus is detectable which is considered a correlate with the time a patient is infectious. Reducing duration of detectable virus thereby impacts transmission dynamics and risk to other within a population, but also may impact on the duration of isolation, containment or hospitalization of a patient, even if it does not correlate directly with individual patient’s signs and symptoms.

Epithelial Cells Infected:

The number of epithelial target cells, T , that are infected (cells/mL) by virus. This metric summarizes the damage to host lung epithelial host cells during the course of infection, and is considered a proxy for the degree of pulmonary inflammatory response and lung tissue damage, and hence pulmonary clinical signs and symptoms within an individual patient. There is increasing evidence that other tissues and organs may be infected by SARS-CoV-2, but those are out-of-scope for this model.

These endpoints were compared to the reference case of the natural history, and expressed as the metric:

$$\log_{10}(\text{Treatment Metric} / \text{No-Treatment Metric})$$

Therefore, a difference of 1 unit of a metric between two treatments indicates an order-of-magnitude change (i.e. a decibel scale).

The 1, 2, 3 target interventions with the best metric at each treatment initiation time, endpoint and summed drug effect was tabulated. Other treatments within 5% of the optimal treatment were also reported and sorted by metric quality.

Results

Figure 2 reports the overview of treatment effects by intervention time and disease metric. The major points from this overview are:

1. Outcome improves for every disease metric with earlier intervention. This suggests that PrEP- and PEP provides the best opportunity for repurposed drugs with (potentially) low potency to impact disease.
2. Treatment initiated after viral peak have little to no impact on viral load AUC. Treatments initiated 3 days after viral peak have no impact on Epithelial Cells Infected. Treatments initiated after viral peak still have potential to shorten the Duration of viral shedding.
3. Combinations targeting multiple pathways can be as effective or more effective as targeting single pathways with equivalent summed treatment effects. The heterogeneity observed at each summed effect level suggests that some combinations are less effective than others.

Figure 3 compares all 1 and 2 target treatments by treatment initiation time (Peak -3, 0, +3 days), endpoint, and 1 and 2 log10 summed drug effect. Supplemental 2 reports results for all combinations. All endpoints are improved with earlier intervention. The major points from this presentation are:

- No endpoints are improved with single or combination treatments targeting k except in the cases of early (Peak -3) intervention with potent (2 log10 summed drug effect). That is, treatments only *delaying* the transition time between cell infection and production of new virions are not generally effective.
- Viral load AUC is improved with single or combination treatments targeting c ; δ and ρ are interchangeable and modestly effective. Single or combination treatments involving β are not effective at or after viral peak.
- Duration of viral shedding is improved with single or combination treatments targeting δ , ρ and c are interchangeable and modestly effective. Single or combination treatments involving β are not effective at or after viral peak.
- Epithelial Cells Infected is improved with single or combination treatments targeting β or c and are interchangeable; δ and ρ are interchangeable and modestly effective.

Table 1 provides a qualitative ranking of target choices by metric of interest. Slowing transition, k , of infected epithelial cells from eclipse, I_1 , to productive, I_2 , is not effective relative to other target choices. Increasing turn-over, δ , and/or decreasing productivity, ρ , of infected epithelial cells, I_2 , is predicted to have positive benefit for all metrics and should be considered a “backbone” of proposed combinations. Broadly speaking, targeting δ and ρ seek to disrupt the production machinery of SARS-CoV-2. Increasing virion kill, c , to deplete extracellular virions, V , is predicted to have positive benefit for all metrics. Inhibiting infection, β , is interchangeable with c for the Epithelial Cells Infected metric, but not the viral load AUC and Duration of viral shedding: c both removes virions and prevents infection but β only prevents infection.

Supplemental Figure 3 and Figure 4 report the predicted impact viral and infected epithelial cell kinetics assuming intervention six days before and six days after peak viral load, respectively.

Discussion

We have argued that the selectivity of anti-viral therapy can be significantly enhanced by exploiting matching of the drug based on its purported mechanism of action with the viral cell cycle dynamics. **Table 2** summarizes the association of the mechanism of action of currently tested repurposed molecules for COVID-19 with the specific rate constants. It is interesting to note that of these drugs, those drugs that target the conversion rate constant alone, such as those that target viral proteolysis, RNA dependent RNA polymerase, and those that act nonspecifically such as ivermectin, cyclosporine and nitroloxanide are least likely to result in meaningful efficacy based on the model described in this manuscript. This is supported by weight of evidence (clinical trial or white paper based arguments) that has been generated so far on remdesivir [7, 8], protease inhibitors [20], and ivermectin [21], that either indicates that the effects are likely to be negligible to modest at best.

Our simulations demonstrated some important themes for consideration of combination treatments targeting the SARS-CoV-2 cell cycle. In general, antivirals should be initiated as early in the course of infection as possible to maximize impact on viral load AUC, duration of viral shedding and number of epithelial cells infected. This was a common theme across the scenarios and endpoints evaluated. Indeed, beginning treatment beyond 3 days after peak viral load is unlikely to have any meaningful impact on endpoints that may correlate with patient symptoms according to our simulations, but benefit for later intervention may persist beyond for clinical and public health endpoints associated with duration of viral shedding. As prolonged viral shedding phenotypes are described for influenza [22] and COVID-19 [23], we performed sensitivity analyses with c and δ . We observed in prolonged viral shedder phenotypes that cessation of viral shedding benefit persists for therapeutics that promote virion kill (c), infected cell death (δ) and inhibit virion release (ρ). Such interventions would be preferred to address so-called SARS-CoV-2 super spreaders [24, 25].

To illustrate the potential benefit of combinations of repurposed drugs, example combinations were drawn from the current trial literature (**Table 3**).

We assumed modest effect (0.333 log10 effect, 53.6% inhibition, 1.15 fold increase) for each target. Single target interventions were selected as β , δ , ρ , c ; two target intervention was selected as $\delta\rho$; three target interventions were selected as $\delta\rho c$ and $\beta\delta\rho$; four target interventions was selected as $\beta\delta\rho c$. **Figure 4** shows the output of these simulations at different intervention times. Supplemental Figure3 and

Figure 4A shows the predicted impact on viral and infected epithelial cell kinetics assuming intervention three days before peak viral load. For the single interventions (top row) β , δ , ρ , c , no single intervention is sufficient to halt viral growth, but each blunts the peak and may shift the timing of peak viral load. However, a meaningful ($> 2 \log_{10}$) improvement in epithelial cells infected is expected. The combination interventions (bottom row) $\delta\rho$, $\beta\delta\rho$, $c\delta\rho$, $\beta\delta\rho c$ follow. The two-target intervention, $\delta\rho$, shows a similar “blunting and delaying” quality on viral load as the single-target interventions, but better overall suppression of viral load and epithelial cell infection. In contrast, the three- and four-target interventions halt viral growth and (nearly) abolish epithelial cell infection. As a reminder, each element of each intervention is assumed to have a modest effect, so the results shown for the multiple-target combinations express their cooperative/synergistic effect on viral load and infected epithelial cells.

Figure 4B shows the predicted impact on viral and infected epithelial cell kinetics assuming intervention at peak viral load. As above, the single interventions have modest effect on viral load, with δ identified as ideal for reducing duration of viral shedding and c identified as ideal for reducing viral load AUC (**Table 1**). A three log₁₀ reduction in uninfected epithelial cells is expected. The three- and four-target interventions somewhat improve duration of viral shedding, but the biggest gain is observed in a one log₁₀ improvement in uninfected epithelial cells, with β identified as ideal for reducing infected epithelial cells (**Table 1**).

Figure 4C shows the predicted impact on viral and infected epithelial cell kinetics assuming intervention three days before peak viral load. Some modest gains are possible for duration of viral shedding, with δ identified as ideal for reducing duration of viral shedding and c identified as ideal for reducing viral load AUC (**Table 1**). Very little improvement in infected epithelial cells is predicted, reinforcing the primary finding of this work and others that early intervention is critical. Here, we explicitly report the effect on host cell damage, which has been underappreciated in prior efforts.

Table 1 captures the primary results of this simulation study, reporting that interventions targeting the host-cell “factories” *for de novo* virions are broadly effective in reducing the magnitude of viral load and infected epithelial cells and reducing the duration of viral shedding. Mechanisms that promote infected cell death (δ) and/or reduce copies of virions per infection (ρ) achieve this goal. Simulations results suggest interchangeability of these effects, with the noted exception of reducing duration of viral shedding where δ is superior to ρ . Interchangeability suggests additive effects, from simplistic anergy/additivity/synergy perspective, but also offers an opportunity to combine two low-potency agents, each targeting one mechanism, to boost the overall potency of the combination. Within the host cells, simply delaying the viral replication machinery (k) is not a good strategy.

Outside or on the border of host cells, **Table 1** reports differing strategies that depend on the objective of the intervention. Mechanisms that remove circulating virus (c) are broadly effective in reducing the viral load AUC and infected epithelial cells and reducing the duration of viral shedding. Mechanisms that prevent viral entry and infection of host cells (β) are only effective prior to peak viral load or if only focused on sparing host cell infection. Put simply, killing virus (c) both removes virus and prevents infection. Vaccines and antibodies fall into the category of removing circulating virus (c), and are predicted to have strong effects even at low potency if administered early (or before, in the case of vaccines) in the course of infection.

Given that the full time course is rarely measured in clinical evaluations with the exception of PEP studies, viral load AUC is a largely insensitive endpoint to evaluate potential therapeutic interventions. This is because of their dependence on the pre-intervention viral load values. For a therapeutic intervention to work in this regard, it needs to exhibit a rapid pharmacological onset (e.g., loading dose, direct rather than indirect pharmacology) and needs to be effective at clearing the virus. Treatments targeting c (killing of released virions) were the most effective, meaning that interventions like convalescent plasma, or investigational antibodies would be anticipated to be most likely to impact total viral load meaningfully.

Of the therapies being investigated, remdesivir was recently shown in hospitalized adults with moderate disease to provide a 31% faster time to recovery than those who received placebo ($p < 0.001$) [8], but no virologic information was reported. However, in the study by Wang et al. [7], remdesivir had no meaningful effect on viral load. Remdesivir is thought to play a role in the incorporation into new viral RNA, leading to the inability of the viral polymerase to add new RNA. In the absence of key mechanistic information, we assumed that remdesivir reduces the production of new virions by halting replication of its genome, and thus its effect is proximally associated with ρ . It is possible that remdesivir may show meaningful efficacy if studied in more early infection phase. Future data on remdesivir in early onset mild patients with COVID-19, combined with suitable therapeutics will likely inform on the benefits of early intervention for this molecule.

Duration of viral shedding is less time sensitive to perturbation than viral load AUC and epithelial cells infected and is also influenced by a broader array of pharmacological interventions in the SARS-CoV2 cell cycle. Unlike both epithelial cells and viral load AUC, treatments targeting δ (death of infected cells) were the most effective against duration of viral shedding. The concept of early intervention with combination

treatments targeting δ was validated in the clinic recently, where an open label, prospective, randomized early treatment study (median 5 days, [IQR 3-7 days] since symptom onset) showed triple combination of ribavirin, lopinavir/ritonavir, interferon (which all target δ) reduced viral shedding by 5 days sooner versus Lop/r alone [9]. Such findings may translate into meaningful benefits for patients and society, as duration of viral shedding may impact duration of hospital stay or isolation for an individual, and risk of transmission to others and the associated costs from a public health perspective [17].

The SARS-CoV-2 cell cycle provides some foundational basis for the selection of existing treatments with pharmacological plausibility within a set of combination regimens. To maximize sparing of epithelial cells and potential consequences of downstream cytotoxicity and pulmonary inflammation, a treatment regimen should include treatment(s) that maximize pharmacology on β (inhibition of new epithelial cell infection) like camostat, chloroquine and hydroxychloroquine, or influence ρ as evidenced via remdesivir. To reduce duration of viral shedding, treatment regimens should include components that effectively reduce δ (death of infected cells) such as ribavirin, lopinavir/ritonavir and/or interferon. Interventions like convalescent plasma, or investigational antibodies such as RGN-COV2 and other investigational antibody treatments targeting c (killing of released virions) have the most significant promise in rapidly reducing viral load and will be a welcome addition to the combination armamentarium.

Future directions

Our model-informed analysis underscores the need to include the key features of the viral cell cycle from the perspective of dynamic models to leverage the significance of cell-cycle checkpoints (vis-à-vis specific rate constants) for emerging therapeutics. Our model builds upon previously described models by extending their utility into assessment of the value of combinations. Such an approach will be invaluable for clinicians and trialists to develop informed hypotheses based on cell cycle selectivity and specificity. The fundamental premise for this approach assumes that cell kinetics and durability of response are intricately regulated and can only be disrupted by a drug that has the specificity for that particular phase.

The model leveraged here is parsimonious and offers a quick, reliable method to triage therapeutics entering clinical assessment for the ongoing pandemic. Efforts are ongoing to further build in wet-lab inputs on the virus characterization model including replication dynamics, tropism and cell culture susceptibility, but also integrating with drug characterization (including ADME profiles), and emerging clinical data from ongoing studies. We hope that further refinements as well as extension to broader incorporation of the downstream host inflammatory response and associated interventions such as immunomodulators including IL-6 inhibitors, will provide a comprehensive disease model backbone that could be fungible for inputting emerging virus pathogens. We believe that a comprehensive quantitative and systems pharmacology approach linking to wet-lab for emerging viruses, can provide a structured scientific back-bone that could revolutionize and rationalize our approach to selecting therapeutic interventions for future pandemics.

Conclusions

The simulation work presented here leverages the known kinetics of the SARS-CoV-2 life cycle to rank potential targeted approaches with a focus on the likely need to combine repurposed, low-potency agents. These simulations suggest early intervention is critical and targeting multiple points important to viral replication within and release from infected host cells is a good strategy for reducing both viral load and host cell infection. In addition, we observed that the time-window opportunity for a therapeutic intervention to effect duration of viral shedding exceeds the effect on sparing epithelial cells from infection or impact on viral load AUC. Furthermore, the impact on reduction on duration of shedding may extend further in patients who exhibit a prolonged shedder phenotype.

Acknowledgements

The authors acknowledge the review of the work by Dr Jeremie Guedj of INSERM and Drs Patrick Smith and Kashyap Patel of Certara. The authors are grateful to Jim Gallagher of Certara in the generation of the graphic.

The authors acknowledge review of the work from Drs Dan Hartman and Steve Kern from the Bill and Melinda Gates Foundation and financial support from the Bill and Melinda Gates Foundation.

References

1. JHU Johns Hopkins University Coronavirus Resource Center. URL: <https://coronavirus.jhu.edu/> (last accessed: May 28, 2020).
2. Guo YR, Cao QD, Hong ZS, Tan YY, Chen SD, Jin HJ, Tan KS, Wang DY, Yan Y. The origin, transmission and clinical therapies on coronavirus disease 2019 (COVID-19) outbreak - an update on the status. *Mil Med Res.* 2020 Mar 13;7(1):11.
3. Phelan AL, Katz R, Gostin LO. The novel coronavirus originating in Wuhan, China: challenges for global health governance. *JAMA* 2020; published online Jan 30. DOI:10.1001/jama.2020.1097.
4. WHO. Coronavirus disease 2019 (COVID-19) situation report–107. May 6, 2020. <https://www.who.int/docs/default-source/coronaviruse/situation-reports/20200506COVID-19-sitrep-107>.
5. Siddiqi H, Mehra M. COVID-19 illness in native and immunosuppressed states: A clinical-therapeutic staging proposal. *J Heart Lung Transplant.* 2020 May;39(5):405-407.
6. Gautret P, Lagier JC, Parola P, et al. Hydroxychloroquine and azithromycin as a treatment of COVID-19: results of an open-label non-randomized clinical trial. *Int J Antimicrob Agents* 2020; published online March 20. DOI:10.1016/j.ijantimicag.2020.105949.
7. Wang Y, Zhang D, Du G, Du R, Zhao J, Jin Y, Fu S, Gao L, Cheng Z, Lu Q, Hu Y, Luo G, Wang K, Lu Y, Li H, Wang S, Ruan S, Yang C, Mei C, Wang Y, Ding D, Wu F, Tang X, Ye X, Ye Y, Liu B, Yang J, Yin W, Wang A, Fan G, Zhou F, Liu Z, Gu X, Xu J, Shang L, Zhang Y, Cao L, Guo T, Wan Y, Qin H, Jiang Y, Jaki T, Hayden FG, Horby PW, Cao B, Wang . Remdesivir in adults with severe COVID-19: a randomized, double-blind, placebo-controlled, multicenter trial. *Lancet.* 2020 May 16;395(10236):1569-1578.
8. Beigel JH, Tomashek KM, Dodd LE, Mehta AK, Zingman BS, Kalil AC, Hohmann E, Chu HY, Luetkemeyer A, Kline S, Lopez de Castilla D, Finberg RW, Dierberg K, Tapson V, Hsieh L, Patterson TF, Paredes R, Sweeney DA, Short WR, Touloumi G, Lye DC, Ohmagari N, Oh MD, Ruiz-Palacios GM, Benfield T, Fatkenheuer G, Kortepeter MG, Atmar RL, Creech CB, Lundgren J, Babiker AG, Pett S, Neaton JD, Burgess TH, Bonnett T, Green M, Makowski M, Osinusi A, Nayak S, Lane HC; ACTT-1 Study Group Members. Remdesivir for the Treatment of COVID-19 - Preliminary Report. *N Engl J Med.* 2020 May 22;NEJMoa2007764. doi: 10.1056/NEJMoa2007764.
9. Hung IF, Lung KC, Tso EY, Liu R, Chung TW, Chu MY, Ng YY, Lo J, Chan J, Tam AR, Shum HP, Chan V, Wu AK, Sin KM, Leung WS, Law WL, Lung DC, Sin S, Yeung P, Yip CC, Zhang RR, Fung AY, Yan EY, Leung KH, Ip JD, Chu AW, Chan WM, Ng AC, Lee R, Fung K, Yeung A, Wu TC, Chan JW, Yan WW, Chan WM, Chan JF, Lie AK, Tsang OT, Cheng VC, Que TL, Lau CS, Chan KH, To KK, Yuen KY. Triple combination of interferon beta-1b, lopinavir–ritonavir, and ribavirin in the treatment of patients admitted to hospital with COVID-19: an open-label, randomised, phase 2 trial. *Lancet* Published Online May 8, 2020. [https://doi.org/10.1016/S0140-6736\(20\)31042-4](https://doi.org/10.1016/S0140-6736(20)31042-4).
10. Nowak MA, Bonhoeffer S, Hill AM, Boehme R, Thomas HC, McDade H. Viral dynamics in hepatitis B virus infection. *Proc. Natl. Acad. Sci. U.S.A.* 1996; 93, 4398–4402. doi: 10.1073/pnas.93.9.4398.
11. Bonhoeffer S, May RM, Shaw GM, Nowak MA. Virus dynamics and drug therapy. *Proc. Natl. Acad. Sci. U.S.A.* 1997; 94, 6971–6976. doi: 10.1073/pnas.94.13.6971.
12. Bocharov GA, Romanyukha AA. Mathematical model of antiviral immune response. *J Theor Biol* 1994; 167: 323-360.
13. Baccam P, Beauchemin C, Macken CA, Hayden FG, Perelson AS. Kinetics of Influenza A Virus Infection in Humans. *J Virol.* 2006 Aug;80(15):7590-9. doi: 10.1128/JVI.01623-05.

14. Goncalves A, Bertrand J, Ke R, Comets E, de Lamballerie X, Malvy D, Pizzorno A, Terrier O, Calatrava MR, Mentre F, Smith P, Perelson AS, Guedj J. Timing of antiviral treatment initiation is critical to reduce SARS Cov-2 viral load. medRxiv preprint doi: <https://doi.org/10.1101/2020.04.04.20047886>.
15. Hu Y, Lu S, Song Z, Wang W, Hao P, Li J, Zhang X, Yen HL, Shi B, Li T, Guan W, Xu L, Liu Y, Wang S, Zhang X, Tian D, Zhu Z, He J, Huang K, Chen H, Zheng L, Li X, Ping J, Kang B, Xi X, Zha L, Li Y, Zhang Z, Peiris M, Yuan Z. Association between adverse clinical outcome in human disease caused by novel influenza A H7N9 virus and sustained viral shedding and emergence of antiviral resistance. *Lancet* 2013; 381 (9885), P2273-2279.
16. Zheng S, Fan J, Yu F, Feng B, Lou B, Zou Q, Xie G, Lin S, Wang R, Yang X, Chen W, Wang Q, Zhang D, Liu Y, Gong R, Ma Z, Lu S, Xiao Y, Gu Y, Zhang J, Yao H, Xu K, Lu X, Wei G, Zhou J, Fang Q, Cai H, Qiu Y, Sheng J, Chen Y, Liang T. Viral load dynamics and disease severity in patients infected with SARS-CoV-2 in Zhejiang province, China, January-March 2020: retrospective cohort study. *BMJ*. 2020 Apr 21;369:m1443.
17. Kamal MA, Smith PF, Chaiyakunapruk N, Wu DB, Pratoomsot C, Lee KK, Chong HY, Nelson RE, Nieforth K, Dall G, Toovey S, Kong DCM, Kamauu A, Kirkpatrick CM, Rayner CR. Interdisciplinary pharmacometrics linking oseltamivir pharmacology, influenza epidemiology and health economics to inform antiviral use in pandemics. *Br J Clin Pharmacol*. 2017;83(7):1580–94.
18. Lovern M, Minton SK, Patel K, Xiong Y, Kirkpatrick CM, Smith PF. Applications of Influenza Viral Kinetic Modeling in Drug Development. *Curr Pharmacol Rep*. 2017; 3 , 294–300.
19. CDC. CDC 2019–Novel Coronavirus (2019-nCoV) Real-Time RT-PCR Diagnostic Panel. Centers for Disease Control and Prevention. 2020 (URL: <https://www.fda.gov/media/134922/download>).
20. Cao B, Wang Y, Wen D, Liu W, Wang J, Fan G, Ruan L, Song B, Cai Y, Wei M, Li X, Xia J, Chen N, Xiang J, Yu T, Bai T, Xie X, Zhang L, Li C, Yuan Y, Chen H, Li H, Huang H, Tu S, Gong F, Liu Y, Wei Y, Dong C, Zhou F, Gu X, Xu J, Liu Z, Zhang Y, Li H, Shang L, Wang K, Li K, Zhou X, Dong X, Qu Z, Lu S, Hu X, Ruan S, Luo S, Wu J, Peng L, Cheng F, Pan L, Zou J, Jia C, Wang J, Liu X, Wang S, Wu X, Ge Q, He J, Zhan H, Qiu F, Guo L, Huang C, Jaki T, Hayden FG, Horby PW, Zhang D, Wang C. A trial of lopinavir-ritonavir in adults hospitalized with severe COVID-19. *N Engl J Med*. 2020 May 7;382(19):1787-1799.
21. Bray M, Rayner C, Noel F, Jans D, Wagstaff K. Ivermectin and COVID-19: A Report in Antiviral Research, Widespread Interest, an FDA Warning, Two Letters to the Editor and the Authors' Responses. *Antiviral Res*. 2020 Apr 21;178:104805. doi: 10.1016/j.antiviral.2020.104805.
22. Giannella M, Alonso M, Garcia de Viedma D, Lopez Roa P, Catalan P, Padilla B, Munoz P, Bouza E. Prolonged viral shedding in pandemic influenza A (H1N1): clinical significance and viral load analysis in hospitalized patients. *Clin Microbiol Infect*. 2011;17(8):1160-1165. doi:10.1111/j.1469-0691.2010.03399.x
23. Li J, Zhang L, Liu B, Song D. Case Report: Viral Shedding for 60 Days in a Woman with COVID-19. *Am J Trop Med Hyg*. 2020;102(6):1210-1213. doi:10.4269/ajtmh.20-0275.
24. Wong G, Liu W, Liu Y, Zhou B, Bi Y, Gao GF. MERS, SARS, and Ebola: The Role of Super-Spreaders in Infectious Disease. *Cell Host Microbe*. 2015;18(4):398-401. doi:10.1016/j.chom.2015.09.013.
25. Cave E. COVID-19 Super-spreaders: Definitional Quandaries and Implications [published online ahead of print, 2020 May 16]. *Asian Bioeth Rev*. 2020;1-8. doi:10.1007/s41649-020-00118-2.
26. Vincent MJ, Bergeron E, Benjannet S, Erickson BR, Rollin PE, Ksiazek TG, Seidah NG, Nichol ST. Chloroquine is a potent inhibitor of SARS coronavirus infection and spread. *Virol J*. 2005 Aug 22;2:69.
27. Hoffmann M, Kleine-Weber H, Schroeder S, Kruger N, Herrler T, Erichsen S, Schiergens TS, Herrler G, Wu NH, Nitsche A, Muller MA, Drosten C, Pohlmann S. SARS-CoV-2 Cell Entry Depends on ACE2 and TMPRSS2 and Is Blocked by a Clinically Proven Protease Inhibitor. *Cell*. 2020 Apr 16;181(2):271-280.e8.

28. Yamamoto M, Matsuyama S, Li X, Takeda M, Kawaguchi Y, Inoue JI, Matsuda Z. Identification of Nafamostat as a Potent Inhibitor of Middle East Respiratory Syndrome Coronavirus S Protein-Mediated Membrane Fusion Using the Split-Protein-Based Cell-Cell Fusion Assay. *Antimicrob Agents Chemother.* 2016 Oct 21;60(11):6532-6539.
29. Liu J, Cao R, Xu M, Wang X, Zhang H, Hu H, Li Y, Hu Z, Zhong W, Wang M. Hydroxychloroquine, a less toxic derivative of chloroquine, is effective in inhibiting SARS-CoV-2 infection in vitro. *Cell Discov.* 2020 Mar 18;6:16.
30. Zhou D, Dai SM, Tong Q. COVID-19: a recommendation to examine the effect of hydroxychloroquine in preventing infection and progression. *J Antimicrob Chemother.* 2020 Mar 20:dkaa114.
31. Prajapat M, Sarma P, Shekhar N, Avti P, Sinha S, Kaur H, Kumar S, Bhattacharyya A, Kumar H, Bansal S, Medhi B. Drug targets for corona virus: A systematic review. *Ind J Pharmacol.* 2020 Jan-Feb; 52(1): 56–65.
32. Baron SA, Devaux C, Colson P, Raoult D, Rolain JM. Teicoplanin: an alternative drug for the treatment of coronavirus COVID-19? *Int J Antimicrob Agents* 2020 Mar 13 : 105944.
33. Falzarano D, de Wit E, Martellaro C, Callison J, Munster VJ, Feldmann H. Inhibition of novel β coronavirus replication by a combination of interferon- α 2b and ribavirin. *Sci Rep* 2013; 3: 1686.
34. Sallard E, Lescure FX, Yazdanpanah Y, Mentre F, Peiffer-Smadja N. Type 1 interferons as a potential treatment against COVID-19. *Antiviral Res.* 2020 Jun; 178: 104791.
35. Gielen V, Johnston SL, Edwards MR. Azithromycin induces anti-viral responses in bronchial epithelial cells. *Eur Resp J.* 2010 Sep;36(3):646-54.
36. Badley AD. In vitro and in vivo effects of HIV protease inhibitors on apoptosis. *Cell Death Differentiation* 2005; 12, 924–931.
37. Schlosser SF, Schuler M, Berg CP, Lauber K, Schulze-Osthoff K, Schmahl FW, Wesselborg S. Ribavirin and Alpha Interferon Enhance Death Receptor-Mediated Apoptosis and Caspase Activation in Human Hepatoma Cells. *Antimicrob Agents Chemother.* 2003 Jun; 47(6): 1912–1921.
38. Patick AK, Potts KE. Protease Inhibitors as Antiviral Agents. *Clin Microbiol Rev.* 1998 Oct; 11(4): 614–627.
39. Tran DH, Sugamata R, Hirose T, Suzuki S, Noguchi Y, Sugawara A, Ito F, Yamamoto T, Kawachi S, Akagawa KS, Omura S, Sunazuka T, Ito N, Mimaki M, Suzuki K.. Azithromycin, a 15 membered macrolide antibiotic, inhibits influenza A (H1N1)pdm09 virus infection by interfering with virus internalization process. *J Antibiot (Tokyo).* 2019 Oct;72(10):759-768.
40. Fehr AR, Perlman S. Coronaviruses: an overview of their replication and pathogenesis. *Methods Mol Biol* 2015; 1282, 1-23.
41. Dong L, Hu S, Gao J. Discovering drugs to treat coronavirus disease 2019 (COVID-19). *Drug Discov Ther* 2020; 14, 58-60.
42. Martinez MA. Compounds with therapeutic potential against novel respiratory 2019 coronavirus. *Antimicrob Agents Chemother.* 2020 Apr 21;64(5):e00399-20.
43. de Wilde AH, Zevenhoven-Dobbe JC, van der Meer Y, Thiel V, Narayanan K, Makino S, Snijder EJ, van Hemert MJ. Cyclosporin A inhibits the replication of diverse coronaviruses. *J Gen Virol.* 2011 Nov;92(Pt 11):2542-2548.
44. Mastrangelo E, Pezzullo M, De Burghgraeve T, Kaptein S, Pastorino B, Dallmeier K, de Lamballerie X, Neyts J, Hanson AM, Frick DN, Bolognesi M, Milani M. Ivermectin is a potent inhibitor of flavivirus repli-

cation specifically targeting NS3 helicase activity: new prospects for an old drug. *J Antimicrob Chemother.* 2012 Aug;67(8):1884-94.

45. Jasenosky LD, Cadena C, Mire CE, Borisevich V, Haridas V, Ranjbar S, Nambu A, Bavari S, Soloveva V, Sadukhan S, Cassell GH, Geisbert TW, Hur S, Goldfeld AE. The FDA-Approved Oral Drug Nitazoxanide Amplifies Host Antiviral Responses and Inhibits Ebola Virus. *iScience.* 2019 Sep 27;19:1279-1290.

46. Duan K, Liu B, Li C, Zhang H, Yu T, Qu J, Zhou M, Chen L, Meng S, Hu Y, Peng C, Yuan M, Huang J, Wang Z, Yu J, Gao X, Wang D, Yu X, Li L, Zhang J, Wu X, Li B, Xu Y, Chen W, Peng Y, Hu Y, Lin L, Liu X, Huang S, Zhou Z, Zhang L, Wang Y, Zhang Z, Deng K, Xia Z, Gong Q, Zhang W, Zheng X, Liu Y, Yang H, Zhou D, Yu D, Hou J, Shi Z, Chen S, Chen Z, Zhang X, Yang X. Effectiveness of convalescent plasma therapy in severe COVID-19 patients. *Proc Natl Acad Sci U S A.* 2020 Apr 28;117(17):9490-9496.

Table 1. Magnitude of endpoint changes by treatment target

Endpoint	k delay productivity	β inhibit infection	c promote virion kill	δ promote infected cell death	ρ inhibit virion release
Viral Load AUC	-	-	++	+	+
Duration of Viral Shedding	-	-	+	++	+
Epithelial Cells Infected	-	++	++	+	+

Table 2. Association of the MOA of the currently tested drugs with the cell cycle components

Cell cycle phase	Mechanism	Example drugs	References
β , Target Cell [Infection] Rate at which circulating virions convert healthy epithelial cells to “eclipse” (non-productive or pre-productive) phase infected cells.	Attachment phase	Camostat and nafamostat to TMPRSS2 Chloroquine to ACE2	26-28
	Endosomal acidification	Chloroquine and hydroxychloroquine, niclosamide	26, 29, 30
	Cytoplasmatic assembly cleavage of viral spike protein by cathepsin L	Leflunomide Teicoplanin	31 32
δ , Productive Cell [Death] Rate at which productively infected cells die.	Programmed cell death, apoptosis, stress response	Interferon azithromycin	33-35
	Apoptosis	protease inhibitors, ribavirin	36, 37

Cell cycle phase	Mechanism	Example drugs	References
p , Virion [Release] Rate at which productively infected cells produce new virions	Unknown	combination treatment (interferons and protease inhibitors) azithromycin	38, 39
	viral proteolysis	lopinavir, ritonavir, nelfinavir, darunavir, bocepravir, ribavirin	40, 41
	RNA-dependent RNA polymerase Nonspecific	remdesivir, favipiravir	41, 42
c , Virion [Kill]	Unknown	ivermectin, cyclosporin, nitazoxanide azithromycin	39, 43-45
		Antibodies, convalescent plasma, RGN-COV2	46

Table 3. Example combinations

Viral cell cycle	Example regimens	Comment
p , Virion [Release]	Remdesivir alone [Beigle et al., 2020]	RCT of intravenous remdesivir in adults hospitalized with evidence of lower respiratory tract involvement, showed improved median recovery time of 11 vs 15 days.
c Virion [Kill]	Antibodies, convalescent plasma, vaccines	Under investigation
δ , Productive Cell [Death] p , Virion [Release]	Interferon-b-1b, ribavirin [Hung et al., 2020] Protease inhibitors	Open label, prospective, randomized early treatment study (median 5 days, [IQR 3-7 days] since symptom onset) showed triple combination reduced viral shedding by 5 days sooner versus Lop/r alone
β , Target Cell [Infection] δ , Productive Cell [Death] p , Virion [Release]	Hydroxychloroquine Azithromycin	Small case series with multiple issues with trial design and no comparator group limit inferences on virologic or clinical efficacy (Guatret et al., 2020). Concerns on QT prolongation (Mercurio et al., 2020)
	Remdesivir + Hydroxychloroquine + lopinavir/ritonavir and/or interferon	Potential RDV triple or quad combination antiviral regimen that covers three parts of viral cell cycle

Figure 1 Cell cycle model and associated specific rate constants as target for therapeutics.

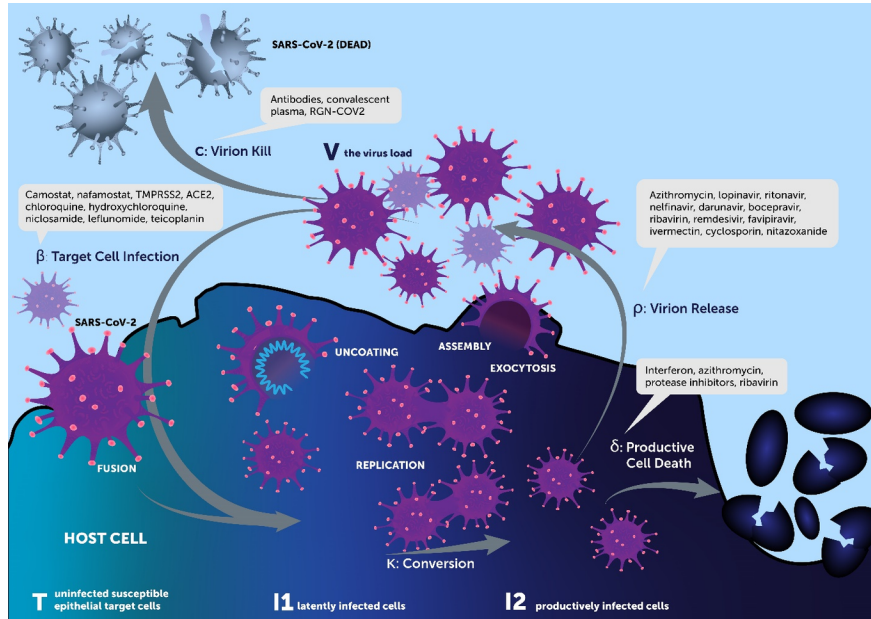
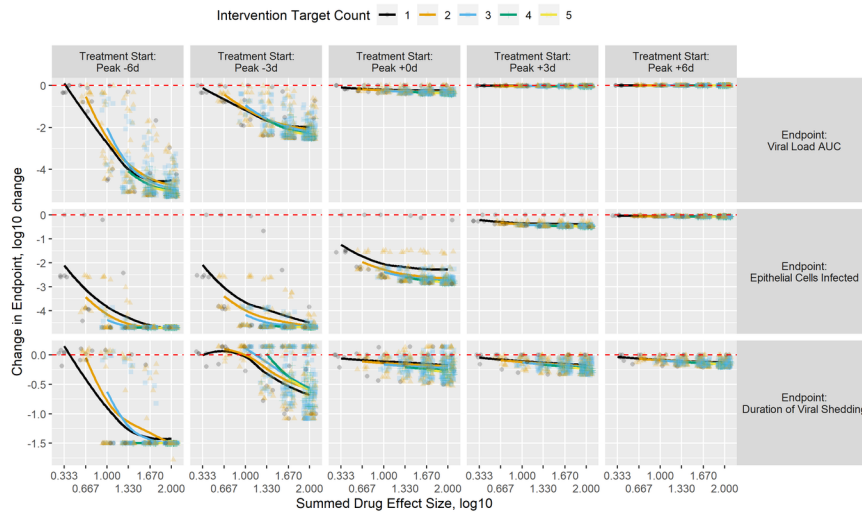
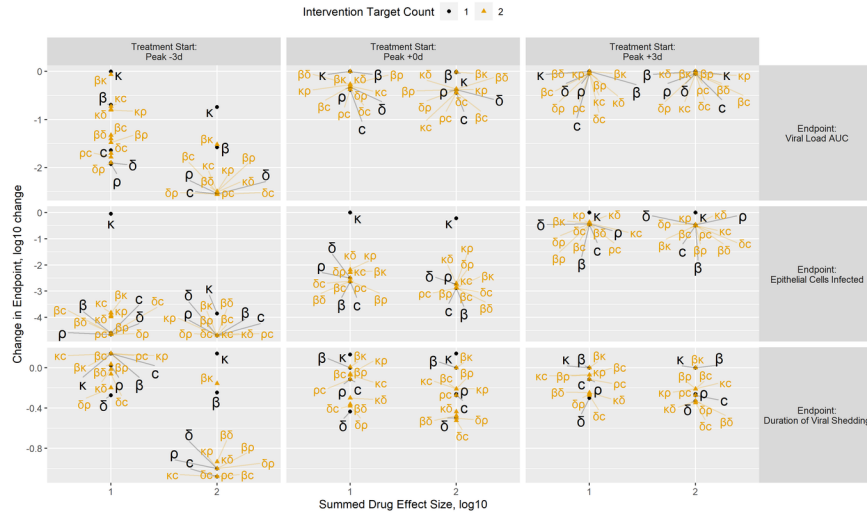


Figure 2. Change in endpoint metrics by treatment start, number of targets in the treatment and summed target effect in the treatment.



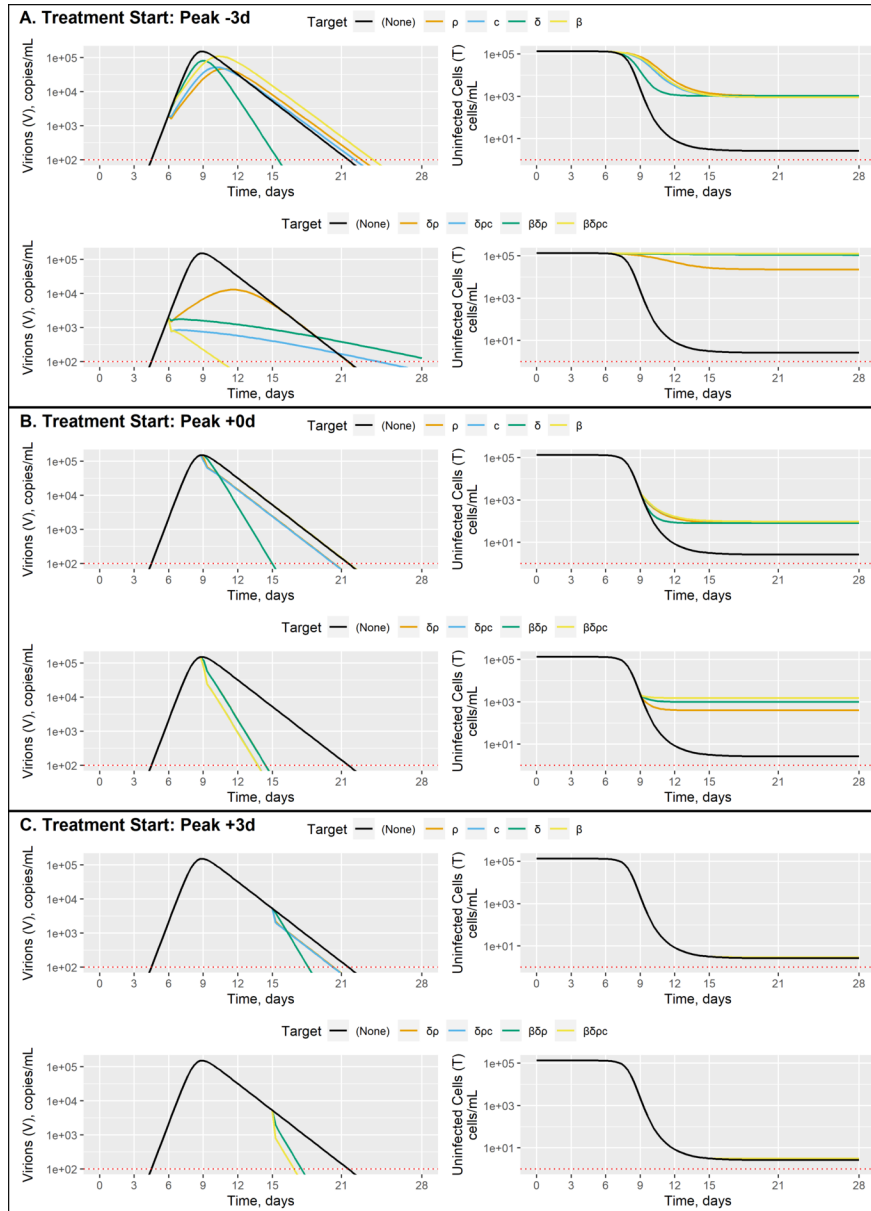
Treatment initiation is shown by column relative to expected viral load peak; endpoint is shown by row; Change in endpoint relative to the no-treatment control is reported on the y-axis as $\log_{10}(\text{treatment outcome metric} / \text{no-treatment outcome metric})$ with negative values representing improvements relative to the no-treatment control; number of targets in each intervention is shown by color and shape; each intervention is plotted by its summed drug effect on the x-axis with some jittering in the x-dimension to aid with overplotting issues; a LOESS smoothing line is added per count of targets to show a general trend of improvement with increasing summed drug effect.

Figure 3. Comparisons of all 1 and 2 target treatments by treatment initiation time, endpoint and summed drug effect.



Treatment initiation is shown by column relative to expected viral load peak; endpoint is shown by row; Change in endpoint relative to the no-treatment control is reported on the y-axis as $\log_{10}(\text{treatment outcome metric} / \text{no-treatment outcome metric})$ with negative values representing improvements relative to the no-treatment control; number of targets in each intervention is shown by color, size and shape; each intervention is plotted by its summed drug effect on the x-axis; labels of the treatment targets appear with lines to connect them to the specific point on the diagram.

Figure 4. Example combination treatments



Interventions initiated 3 days before, at, and 3 days after peak viral count are shown panels A, B, and C, respectively; within each panel, single-target and multiple-target interventions are shown on the top and bottom row, respectively; Virion and Uninfected endpoint is shown by column; Simulation values over time are reported on the y-axis and x-axis, respectively; specific targets are shown by color with the no-intervention (negative control) case shown in black.

